

Inverted tandem organic solar cells with a MoO₃/Ag/Al/Ca intermediate layer

X. W. Sun, D. W. Zhao, L. Ke, A. K. K. Kyaw, G. Q. Lo et al.

Citation: *Appl. Phys. Lett.* **97**, 053303 (2010); doi: 10.1063/1.3469928

View online: <http://dx.doi.org/10.1063/1.3469928>

View Table of Contents: <http://apl.aip.org/resource/1/APPLAB/v97/i5>

Published by the [American Institute of Physics](http://www.aip.org).

Related Articles

Molecular control of photoexcited charge transfer and recombination at a quaterthiophene/zinc oxide interface
[APL: Org. Electron. Photonics 5, 113 \(2012\)](#)

Molecular control of photoexcited charge transfer and recombination at a quaterthiophene/zinc oxide interface
[Appl. Phys. Lett. 100, 203306 \(2012\)](#)

Reevaluation of the beneficial effect of Cu(In,Ga)Se₂ grain boundaries using Kelvin probe force microscopy
[Appl. Phys. Lett. 100, 203903 \(2012\)](#)

Direct and charge transfer state mediated photogeneration in polymer–fullerene bulk heterojunction solar cells
[Appl. Phys. Lett. 100, 193302 \(2012\)](#)

Direct and charge transfer state mediated photogeneration in polymer–fullerene bulk heterojunction solar cells
[APL: Org. Electron. Photonics 5, 106 \(2012\)](#)

Additional information on *Appl. Phys. Lett.*

Journal Homepage: <http://apl.aip.org/>

Journal Information: http://apl.aip.org/about/about_the_journal

Top downloads: http://apl.aip.org/features/most_downloaded

Information for Authors: <http://apl.aip.org/authors>

ADVERTISEMENT



Goodfellow
metals • ceramics • polymers • composites
70,000 products
450 different materials
small quantities fast

www.goodfellowusa.com

Inverted tandem organic solar cells with a MoO₃/Ag/Al/Ca intermediate layer

X. W. Sun,^{1,2,a)} D. W. Zhao,^{1,3,b)} L. Ke,⁴ A. K. K. Kyaw,¹ G. Q. Lo,³ and D. L. Kwong³

¹School of Electrical and Electronic Engineering, Nanyang Technological University, Nanyang Avenue, Singapore 639798

²Department of Applied Physics, College of Science, Tianjin University, Tianjin 300072, China

³Institute of Microelectronics, A*STAR (Agency for Science, Technology and Research), 11 Science Park Road, Science Park II, Singapore 117685

⁴Institute of Materials Research and Engineering, A*STAR (Agency for Science, Technology and Research), 3 Research Link, Singapore 117602

(Received 5 April 2010; accepted 6 July 2010; published online 2 August 2010)

An inverted tandem organic solar cell, consisting of two bulk heterojunction subcells with identical poly(3-hexylthiophene) and 1-(3-methoxycarbonyl)-propyl-1-phenyl-(6,6)C₆₁ active layer, and an intermediate layer made of ultrathin multiple metal layers of Ca/Al/Ag and metal oxide MoO₃, is reported. This intermediate layer is of advantage in high transparency and low series resistance. Moreover, it serves as the charge recombination center effectively, and renders an exact summation of the open-circuit voltages (1.18 V) of the two subcells and a high fill factor (61.8%). The maximum power conversion efficiency obtained is 2.78% under simulated 100 mW/cm² [air mass (AM) 1.5G] solar irradiation, comparable to those of the two subcells. © 2010 American Institute of Physics. [doi:10.1063/1.3469928]

Organic solar cells (OSCs) have been studied intensively as one kind of the third generation solar cells with potentially low cost and flexible form.^{1,2} Although there have been some progresses recently in bulk heterojunction (BHJ) OSCs,³⁻⁵ they are still limited by a few factors associated with essential properties of organic semiconductors, such as narrow absorption range, short exciton diffusion length, and small charge carrier mobility. Tandem structure consisting of two or more cells with complementary absorption spectra,⁶⁻¹² is considered as an effective way to boost the efficiency. Herein, the intermediate layer, connecting the subcells optically and electrically, plays a crucial role in overall device performance.¹⁰ Thus far, quite a few intermediate layers have been reported,¹³ such as Ag nanoclusters,⁶ Au,¹⁴ Al/WO₃,⁸ indium tin oxide (ITO)/poly(3,4-ethylene dioxithiophene):(polystyrene sulfonic acid) (PEDOT:PSS),¹⁵ Al/Au/PEDOT:PSS,⁷ ZnO/PEDOT:PSS,¹⁶ TiO_x/PEDOT:PSS,⁹ Al/MoO₃,¹⁰⁻¹² and Al/TiO₂:Cs/PEDOT:PSS.¹⁷

On the other hand, the inverted structure [with modified ITO on glass as the cathode (at the bottom) and a high work function metal as anode (at the top)] as an important progress in OSCs has been extensively studied recently.^{5,18-21} The conventional BHJ architecture (with ITO on glass as the anode at the bottom and a low work function metal as anode atop) has limitations in device stability due to air-sensitive low-work-function metal cathode such as Al. Diffusion of oxygen into the active layer through pinholes and grain boundaries in Al cathode causes the degradation of the active layer, leading to device instability in air.²² Also, degradation of ITO/PEDOT:PSS interface is inevitable because of slightly acidic nature of PEDOT:PSS.^{22,23} Moreover, the spin-coated P3HT:PCBM active layer exhibits a vertical

phase separation with a concentration gradient changing from PCBM-rich at the bottom (closer to the substrate) to P3HT-rich atop (farther away from the substrate),^{5,24,25} which obstructs charge transport and charge collection in the conventional structure. The inverted structure of organic solar cell (OSC) overcomes the above problems associated with the conventional structure with demonstrated better performance especially in the device lifetime.^{5,23,26}

Thus, combining tandem and inverted structures in one device will benefit in terms of both device efficiency and stability. However, so far, there is no report on such inverted tandem OSC. It is worth mentioning that the “inverted structure” reported in Ref. 9 is still a normal tandem structure with ITO anode at the bottom and low work function cathode atop, in which the inversion refers to swapping the high and low band gap materials. Thus, it is completely different from the inverted tandem structure to be discussed in this paper, where we shall report an inverted tandem cell with an efficient intermediate layer of MoO₃/Ag/Al/Ca.

All cells were fabricated on ITO coated glass substrates with a sheet resistance of 20 Ω/square. A Ca layer was first thermally evaporated in a base vacuum of 9.0×10⁻⁵ Pa. Then, a blend solution made of poly(3-hexylthiophene) (P3HT) (Rieke Metals, Inc.) and 1-(3-methoxycarbonyl)-propyl-1-phenyl-(6,6)C₆₁ (PCBM) (American Dye Sources Inc.) with a weight ratio of 1:0.8 in chlorobenzene (30 mg/mL) was spin-coated to form the active layers for both bottom and top subcells in a glovebox filled with N₂. MoO₃, Ag, Al, and Ca were evaporated in designed sequence and combinations to form the intermediate layer (9.0×10⁻⁵ Pa). Evaporated MoO₃/Ag was used as the anode for all single and tandem cells in this paper. A postannealing at 160 °C for 10 min was always performed for all devices after the final MoO₃/Ag anode fabrication. All devices had an active area of 0.1 cm² and were encapsulated before taking out from the glovebox. The current-voltage (*I-V*) characteristics

^{a)}Electronic-mail: exwsun@ntu.edu.sg.

^{b)}Electronic-mail: dewei_zhao@hotmail.com.

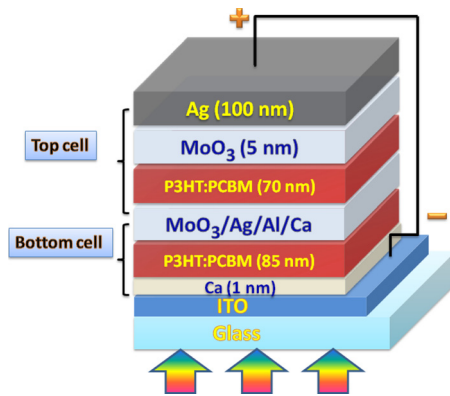


FIG. 1. (Color online) The device structure of the inverted tandem cell with $\text{MoO}_3/\text{Ag}/\text{Al}/\text{Ca}$ intermediate layer.

were measured with a Keithley 2400 sourcemeter under simulated $100 \text{ mW}/\text{cm}^2$ [air mass (AM) 1.5G] irradiation from a solar simulator (Solar Light Co. Inc.). The transmittance spectra of the samples were recorded using UV-VIS-NIR scanning spectrophotometer (UV-3101PC). The film thickness was measured with a surface profiler (Tencor P15). Figure 1 shows the structure of the inverted tandem cell in this study, consisting of ITO/Ca(1 nm)/P3HT:PCBM(85 nm)/intermediate layer/P3HT:PCBM(70 nm)/ MoO_3 (5 nm)/Ag(100 nm). Various intermediate layers, as shown in Fig. 2, were compared.

Figure 2 shows the transmittance spectra of different combinations of intermediate layers and the absorption spectrum of P3HT:PCBM film. Obviously, MoO_3/Ca and $\text{MoO}_3/\text{Al}/\text{Ca}$ have a high transparency of 98% ranging from 300 to 800 nm.^{10,20} With the insertion of Ag (1 nm), the transmittance of $\text{MoO}_3/\text{Ag}/\text{Ca}$ and $\text{MoO}_3/\text{Ag}/\text{Al}/\text{Ca}$ decreases in the range from 400 to 600 nm, exhibiting a transmittance dip peaking at 485 nm. This implies that Ag nanocluster layer (1 nm) is slightly absorptive in this range due to localized surface plasmon resonance (LSPR).^{27–30} However, the LSPR absorption does not occur for either MoO_3/Al or MoO_3/Ca interface. Considering that a postannealing was performed for the devices, it is possible that an oxide layer (O deficient) between MoO_3 and Al (or Ca) is formed since either Al or Ca has a lower electronegativity value than Mo (the Pauling electronegativity of Al, Ca, and Mo is 1.61, 1.00, and 2.16, respectively). Formation of such oxide layer will lead to a reduction in electron density, preventing LSPR

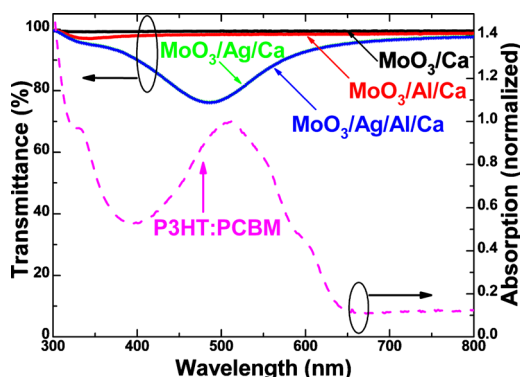


FIG. 2. (Color online) The transmittance spectra of different combinations of intermediate layers: MoO_3 (7.5 nm)/Ca(3 nm), MoO_3 (7.5 nm)/Al(1 nm)/Ca(3 nm), MoO_3 (7.5 nm)/Ag(1 nm)/Ca(3 nm), and MoO_3 (7.5 nm)/Ag(1 nm)/Al(1 nm)/Ca(3 nm), and also the absorption spectrum of the P3HT:PCBM film.

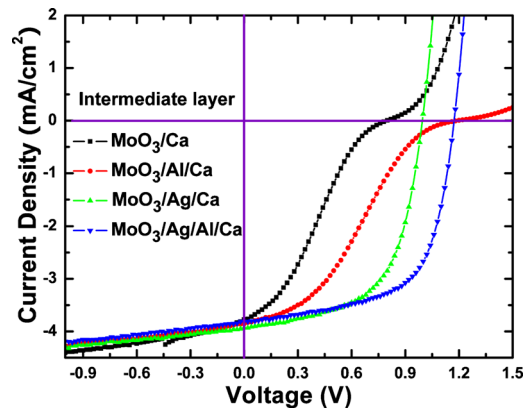


FIG. 3. (Color online) The comparison of the I - V characteristics of the inverted tandem cells with different combinations of intermediate layers.

from happening. Interestingly, the transparency of $\text{MoO}_3/\text{Ag}/\text{Al}/\text{Ca}$ is nearly the same as that of $\text{MoO}_3/\text{Ag}/\text{Ca}$, although 1 nm Al is added in between, demonstrating that the insertion of Al nanocluster layer has no or little effect on the transparency of the intermediate layer. The function of MoO_3 layer can be found elsewhere.^{20,21} It has to be thick enough to protect the prior-deposited polymer layer, yet thin enough not to induce large voltage loss and high series resistance.^{20,21} In our experiment, the optimal thickness of MoO_3 is 7.5 nm.

Figure 3 shows the comparison of the I - V characteristics of the inverted tandem cells with different combinations of intermediate layers. Although the V_{oc} for the cell with MoO_3/Ca intermediate layer approaches 0.79 V, it is much smaller than the V_{oc} summation of two inverted subcells due to large voltage loss across the MoO_3/Ca interface. For regular tandem cell,^{10,17} an ultrathin Al is quite necessary. In the case of inverted tandem cell, the insertion of 1 nm Al between MoO_3 and Ca increases the V_{oc} of inverted tandem cell to 1.19 V, equal to the sum of the V_{oc} values of inverted subcells. However, both inverted tandem cells with MoO_3/Ca and $\text{MoO}_3/\text{Al}/\text{Ca}$ exhibit an S-shaped I - V curve, similar to some previous reports.^{17,31} Such an S-shaped curve may be caused by the formed oxide layer as above-mentioned, which blocks charge extraction and recombination at the intermediate layer, resulting in rather poor fill factors (FFs) (27.9% and 31.2%) for both cells.

In contrast, with 1 nm Ag inserted between Ca (or Al/Ca) and MoO_3 , it is obvious that the S-shaped curve disappears. This indicates that the formation of the oxide layer between MoO_3 and Ca (or Al) is prevented by the insertion of Ag. As a consequence, the FF remarkably roars up to $\sim 60\%$, similar to those of inverted subcells. However, the V_{oc} (0.99 V) of the inverted tandem cell with $\text{MoO}_3/\text{Ag}/\text{Ca}$ is lower than the summation of the V_{oc} 's of the inverted subcells, suggesting the existence of an energy barrier.¹⁷ With an ultrathin Al incorporated between Ag and Ca, an Ohmic contact between both subcells is fully established, leading to removal of the charge extraction/recombination barrier. Hence, the V_{oc} of 1.18 V is obtained for the inverted tandem cell with $\text{MoO}_3/\text{Ag}/\text{Al}/\text{Ca}$, which is almost the exact summation of the V_{oc} 's (0.57 and 0.63 V) of the subcells, demonstrating no voltage loss across the intermediate layer. In addition, the slight increase in FF to 61.8% is ascribed to the fact that Al functions (work functions of Ag, Al, and Ca are 4.4 eV, 4.3 eV, and 2.9 eV, respectively) as an energy step

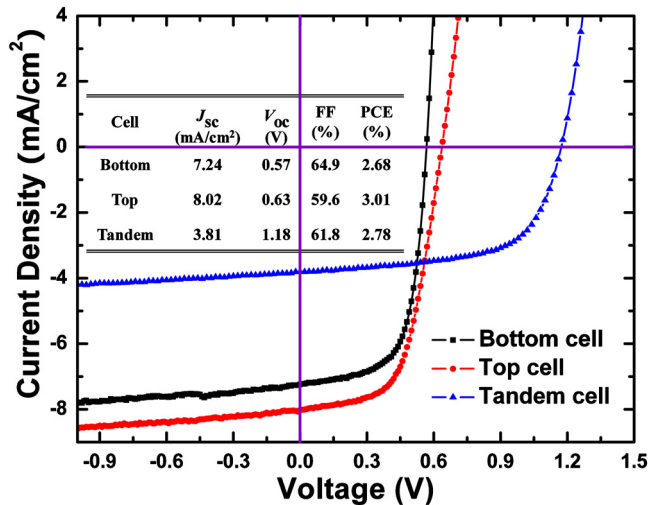


FIG. 4. (Color online) The I - V characteristics of the inverted bottom subcell, top subcell, and tandem cell with $\text{MoO}_3/\text{Ag}/\text{Al}/\text{Ca}$ intermediate layer under $100 \text{ mW}/\text{cm}^2$. The bottom subcell is with a structure of $\text{ITO}/\text{Ca}(1 \text{ nm})/\text{P3HT}:\text{PCBM}(85)/\text{MoO}_3(7.5 \text{ nm})/\text{Ag}$ and the top subcell is with a structure of $\text{ITO}/\text{Ca}(3 \text{ nm})/\text{P3HT}:\text{PCBM}(70 \text{ nm})/\text{MoO}_3(5.0 \text{ nm})/\text{Ag}$. The inset shows the summary of all device performance.

for efficient charge recombination sites of the holes extracted from bottom subcell through MoO_3/Ag and the electrons extracted from top subcell through Ca. Finally, the inverted tandem cell with $\text{MoO}_3/\text{Ag}/\text{Al}/\text{Ca}$ has a power conversion efficiency (PCE) of 2.78% with a J_{sc} of $3.81 \text{ mA}/\text{cm}^2$, V_{oc} of 1.18 V, and FF of 61.8%.

Figure 4 shows the I - V characteristics of inverted bottom subcell, top subcell, and tandem cell with $\text{MoO}_3/\text{Ag}/\text{Al}/\text{Ca}$ intermediate layer under $100 \text{ mW}/\text{cm}^2$. The summarized performance is tabulated as the inset of Fig. 4. The inverted bottom subcell has a PCE of 2.68% with $J_{sc} = 7.24 \text{ mA}/\text{cm}^2$, $V_{oc} = 0.57 \text{ V}$, and $\text{FF} = 64.9\%$. It is worth mentioning that the smaller V_{oc} (0.57 V) is attributed to the voltage loss across the relatively thick MoO_3 layer (7.5 nm).^{20,21} For the inverted top subcell, since a 3 nm thick Ca is used to modify the ITO substrate for electron extraction, there is some slight light loss. As a result, its PCE reaches 3.01% with $J_{sc} = 8.02 \text{ mA}/\text{cm}^2$, $V_{oc} = 0.63 \text{ V}$, and $\text{FF} = 59.6\%$. It is obvious that both inverted subcells have not achieved the best performance,^{20,21} as a relatively thick MoO_3 in bottom subcell protects the prior-deposited polymer layer and a relatively thick Ca in top subcell forms a continuous film to collect electrons from the top subcell and also to avoid “short-circuit” points.

It is noted that the high FF (61.8%) of the inverted tandem cell is comparable to those of inverted single cells, and significantly larger than that of the regular tandem cell.¹⁰ The J_{sc} decreases since identical materials (P3HT:PCBM) are used as the active layer for the subcells. Overall, the PCE (2.78%) of inverted tandem cell is comparable to those (2.68% and 3.01%) of single cells due to the compensation of the doubled V_{oc} .

In conclusions, we have presented an inverted tandem OSC using multiple metal layers $\text{Ag}/\text{Al}/\text{Ca}$ and a metal oxide MoO_3 layer as the intermediate layer. With an optimal intermediate layer, the inverted tandem cell exhibits a PCE

of 2.78% under $100 \text{ mW}/\text{cm}^2$, comparable to those of inverted single subcells. This $\text{MoO}_3/\text{Ag}/\text{Al}/\text{Ca}$ intermediate layer provides an effective and useful approach for further improvement of tandem cell performance.

Financial support from Academic Research Fund (Grant No. RGM 44/06) of Ministry of Education, Singapore is gratefully acknowledged.

¹F. C. Krebs, *Org. Electron.* **10**, 761 (2009).

²F. C. Krebs, *Sol. Energy Mater. Sol. Cells* **93**, 394 (2009).

³W. Z. Cai, X. Gong, and Y. Cao, *Sol. Energy Mater. Sol. Cells* **94**, 114 (2010).

⁴E. Bundgaard and F. C. Krebs, *Sol. Energy Mater. Sol. Cells* **91**, 954 (2007).

⁵L. M. Chen, Z. R. Hong, G. Li, and Y. Yang, *Adv. Mater.* **21**, 1434 (2009).

⁶J. G. Xue, S. Uchida, B. P. Rand, and S. R. Forrest, *Appl. Phys. Lett.* **85**, 5757 (2004).

⁷A. Hadipour, B. de Boer, J. Wildeman, F. B. Kooistra, J. C. Hummelen, M. G. R. Turbiez, M. M. Wienk, R. A. J. Janssen, and P. W. M. Blom, *Adv. Funct. Mater.* **16**, 1897 (2006).

⁸A. G. F. Janssen, T. Riedl, S. Hamwi, H. H. Johannes, and W. Kowalsky, *Appl. Phys. Lett.* **91**, 073519 (2007).

⁹J. Y. Kim, K. Lee, N. E. Coates, D. Moses, T. Q. Nguyen, M. Dante, and A. J. Heeger, *Science* **317**, 222 (2007).

¹⁰D. W. Zhao, X. W. Sun, C. Y. Jiang, A. K. K. Kyaw, G. Q. Lo, and D. L. Kwong, *Appl. Phys. Lett.* **93**, 083305 (2008).

¹¹D. W. Zhao, X. W. Sun, C. Y. Jiang, A. K. K. Kyaw, G. Q. Lo, and D. L. Kwong, *IEEE Electron Device Lett.* **30**, 490 (2009).

¹²D. W. Zhao, W. H. Tang, L. Ke, S. T. Tan, and X. W. Sun, *ACS Appl. Mater. Interfaces* **2**, 829 (2010).

¹³A. Hadipour, B. de Boer, and P. W. M. Blom, *Adv. Funct. Mater.* **18**, 169 (2008).

¹⁴G. Dennler, H. J. Prall, R. Koeppel, M. Egginger, R. Autengruber, and N. S. Sariciftci, *Appl. Phys. Lett.* **89**, 073502 (2006).

¹⁵K. Kawano, N. Ito, T. Nishimori, and J. Sakai, *Appl. Phys. Lett.* **88**, 073514 (2006).

¹⁶J. Gilot, M. M. Wienk, and R. A. J. Janssen, *Appl. Phys. Lett.* **90**, 143512 (2007).

¹⁷S. Sista, M. H. Park, Z. R. Hong, Y. Wu, J. H. Hou, W. L. Kwan, G. Li, and Y. Yang, *Adv. Mater.* **22**, 380 (2010).

¹⁸S. K. Hau, H. L. Yip, H. Ma, and A. K. Y. Jen, *Appl. Phys. Lett.* **93**, 233304 (2008).

¹⁹A. K. K. Kyaw, X. W. Sun, C. Y. Jiang, G. Q. Lo, D. W. Zhao, and D. L. Kwong, *Appl. Phys. Lett.* **93**, 221107 (2008).

²⁰D. W. Zhao, P. Liu, X. W. Sun, S. T. Tan, L. Ke, and A. K. K. Kyaw, *Appl. Phys. Lett.* **95**, 153304 (2009).

²¹D. W. Zhao, S. T. Tan, L. Ke, P. Liu, A. K. K. Kyaw, X. W. Sun, G. Q. Lo, and D. L. Kwong, *Sol. Energy Mater. Sol. Cells* **94**, 985 (2010).

²²M. Jørgensen, K. Norrman, and F. C. Krebs, *Sol. Energy Mater. Sol. Cells* **92**, 686 (2008).

²³S. K. Hau, H. L. Yip, N. S. Baek, J. Y. Zou, K. O'Malley, and A. K. Y. Jen, *Appl. Phys. Lett.* **92**, 253301 (2008).

²⁴Z. Xu, L. M. Chen, G. W. Yang, C. H. Huang, J. H. Hou, Y. Wu, G. Li, C. S. Hsu, and Y. Yang, *Adv. Funct. Mater.* **19**, 1227 (2009).

²⁵M. Campoy-Quiles, T. Ferenczi, T. Agostinelli, P. G. Etchegoin, Y. Kim, T. D. Anthopoulos, P. N. Stavrinou, D. D. C. Bradley, and J. Nelson, *Nature Mater.* **7**, 158 (2008).

²⁶T. Kuwabara, T. Nakayama, K. Uozumi, T. Yamaguchi, and K. Takahashi, *Sol. Energy Mater. Sol. Cells* **92**, 1476 (2008).

²⁷T. Jiang, L. Miao, S. Tanemura, M. Tanemura, G. Xu, and R. P. Wang, *Superlattices Microstruct.* **46**, 159 (2009).

²⁸G. Xu, C. M. Huang, M. Tazawa, P. Jin, and D. M. Chen, *J. Appl. Phys.* **104**, 053102 (2008).

²⁹G. Xu, Y. Chen, M. Tazawa, and P. Jin, *Appl. Phys. Lett.* **88**, 043114 (2006).

³⁰F. C. Chen and C. H. Lin, *J. Phys. D: Appl. Phys.* **43**, 025104 (2010).

³¹D. Cheyns, H. Gommans, M. Odijk, J. Poortmans, and P. Heremans, *Sol. Energy Mater. Sol. Cells* **91**, 399 (2007).